International Journal of Future Engineering Innovations

Kinematic Analysis of a Serial Manipulator Leg for a Spherical Parallel Robot with Three Coaxial Revolute Joints

Le Van Thao
Institute of Automation, Academy of Military Science and Technology, 89B Ly Nam De, Hoan Kiem, Hanoi, Vietnam

* Corresponding Author: **Le Van Thao**

Article Info

ISSN (online): 3049-1215
Volume: 02
Issue: 05
September-October 2025
Received: 13-07-2025
Accepted: 14-08-2025
Published: 08-09-2025
Page No: 18-26

Abstract
This paper presents a detailed kinematic analysis of a single leg of a 3-DOF spherical parallel robot with coaxial input links. The analysis focuses on determining the fundamental quantities, including the position, velocity, and acceleration of the end-effector. Forward kinematics is employed to derive the position and orientation of the spherical platform based on the known input joint angles. To address this problem, the homogeneous transformation matrix method is applied to establish and define the local coordinate frames, thereby constructing a clear geometric relationship between the links and the spherical platform. This approach not only simplifies the computational process but also provides a rigorous foundation for a deeper investigation of the kinematic characteristics of the mechanism.
In addition, the determination of the workspace represents another important aspect of the study. The positional workspace of the end-effector is described as the set of all achievable positions during operation, while its orientation is defined as the direction from the center of rotation to these positions. Through this analysis, the obtained workspace enables the evaluation of motion limits, orientation capability, and the effective range of the mechanism. Such results are essential for validating the practical applicability of the robot in tasks requiring high precision, while also providing valuable data for subsequent studies on dynamics and control system design.

DOI: https://doi.org/10.54660/IJFEI.2025.2.5.18-26

Keywords: Spherical Parallel Robot, Serial Manipulator Leg, Kinematic Model, Workspace.

1. Introduction

Spherical Parallel Robots (SPRs) are a specialized class of robotic mechanisms characterized by their ability to provide three degrees of freedom (3-DoF) of pure rotational motion [1]. This is achieved by connecting a mobile platform to a fixed base via multiple closed-loop kinematic chains, or legs, with all joint axes intersecting at a single, common point known as the center of rotation [2]. This distinctive kinematic feature makes them highly advantageous for applications requiring precise orientation, such as camera mounts, medical instrument alignment, and haptic feedback devices [3].
Within the domain of SPRs, various kinematic architectures have been explored, with a significant number of studies focusing on the 3-RRR type, which utilizes three identical legs composed exclusively of revolute joints [1]. This report addresses a highly specific and particularly advantageous variation of this design: a 3-RRR leg where all three revolute joints are coaxial. The investigation is centered on the forward kinematics and workspace analysis of this single serial leg, a critical building block for the overall parallel robot. The coaxial configuration, a feature of modern designs like the DLR CoaxHaptics-3RRR haptic device, presents a unique case study in mechanism design [4]. The coaxial arrangement of revolute joints is a deliberate and impactful design choice that fundamentally alters the kinematic and performance characteristics of the manipulator. Unlike a generic RRR serial chain, where joint axes are often perpendicular or offset to achieve a large workspace (e.g., an anthropomorphic arm) [5] the coaxial configuration constrains all joint rotations to a single axis. This constraint, while limiting the individual leg's motion to a single rotational dimension, is instrumental in achieving superior performance for the overall parallel robot [6]. This

architectural decision is a strategic trade-off. The coaxial design, which makes the overall mechanism mechanically overdetermined, provides two significant advantages: high rigidity with respect to translational degrees of freedom and a lighter design with reduced rotational inertia.

The kinematic simplicity of the single leg's motion is thus part of a broader engineering solution that prioritizes robust structural and dynamic performance over the kinematic versatility of an open-loop chain. For applications like haptic interfaces, where high stiffness, low inertia, and continuous motion are paramount, this design choice is a direct response to a core engineering challenge. The analysis of the single leg's kinematics, therefore, is not a standalone academic exercise but a foundational step toward understanding the exceptional performance of the complete parallel system [6].

This report is structured to provide a comprehensive and rigorous analysis of the coaxial 3-RRR serial leg. Establishes the kinematic foundations and geometric model, defining the coordinate frames and link parameters. Presents the detailed forward kinematic analysis, offering both a closed-form solution for the single leg and a discussion of its implications for the overall parallel robot. Delves into the workspace analysis, outlining various methods for its determination and exploring the unique shape of the workspace.

2. Materials Characteristics

2.1. Kinematic Analysis

The 3-DOF spherical parallel manipulator (SPM) with a 3-RRR architecture and coaxial actuated input joints is a highly specialized robotic mechanism designed to generate pure rotational motion of its output platform, also known as the wrist. This configuration is widely recognized for its compact structure, high stiffness, and excellent dynamic performance, making it particularly suitable for applications requiring precise orientation control [6-11].

The structural components of this manipulator can be described as follows (Figure 1):

- **Base (1):** The base is the stationary part of the mechanism that provides structural stability and houses the actuators. In the case of the 3-RRR spherical manipulator, the base typically accommodates three coaxially arranged revolute actuated joints. This coaxial arrangement significantly reduces the overall footprint of the mechanism and allows for a more compact integration of actuators. The base also serves as the main reference frame for describing the kinematics and dynamics of the system, ensuring that all subsequent motions are relative to this fixed part.
- **Rotary Plate (2):** The rotary plate, directly connected to the actuated joints, acts as an intermediary link transmitting motion from the actuators to the proximal links. It plays a crucial role in defining the spherical motion workspace, since its orientation dictates how each proximal link is positioned around the common center of rotation. The coaxial design ensures that the rotary plate rotates concentrically around a fixed point, simplifying the geometry of motion analysis and enabling high repeatability in angular positioning.
- **Proximal Link (3):** Each proximal link is a rigid body connected at one end to the rotary plate via a revolute joint. The other end of the proximal link connects to the distal link through a secondary revolute joint. These links act as the first transmission elements in each kinematic chain, translating the rotational input from the actuated joints into constrained motion that drives the distal links. Their geometry is carefully designed to maintain the spherical nature of the workspace, ensuring that all movement is confined to pure orientation around the manipulator’s geometric center.
- **Distal Link (4):** The distal links form the intermediate connections between the proximal links and the moving platform (wrist). Through revolute joints at both ends, the distal links complete each RRR kinematic chain. Their role is to constrain the relative motion of the platform, enforcing the spherical nature of the mechanism. The dimensions of the distal links directly affect the range of motion, singularity distribution, and dexterity of the manipulator. Optimized design of these links ensures smooth transmission of angular velocity and torque, while minimizing undesired mechanical stresses.
- **Wrist (5):** The wrist, or the moving platform, represents the output of the manipulator. It is connected to all three distal links via revolute joints that intersect at a common virtual center. This guarantees that the output motion of the wrist is purely rotational, without any translational component. The wrist is typically used to mount sensors, tools, or end-effectors depending on the application—for example, cameras in vision systems, mirrors in optical alignment devices, or instruments in minimally invasive surgical robots. Its lightweight design is essential for achieving high-speed, precise orientation control while reducing the inertial load on the entire system.

The entire 3-RRR spherical manipulator is designed such that all axes of revolute joints intersect at a single common point, forming a perfect spherical motion center. The coaxial arrangement of actuated input joints provides a mechanically over constrained yet efficient design, which not only enhances the stiffness and accuracy but also reduces the complexity of actuator placement. The manipulator achieves three degrees of freedom corresponding to the rotational motions about three orthogonal axes [12-17].

This architecture offers several advantages:

Compactness: The coaxial arrangement minimizes spatial requirements, enabling integration in confined environments.

Accuracy and Repeatability: The parallel configuration reduces error accumulation compared to serial manipulators.

Stiffness and Load Capacity: The parallel structure distributes loads evenly, improving rigidity and payload-to-weight ratio.

Dynamic Performance: Reduced moving mass in the wrist improves acceleration and velocity responses, making it ideal for high-speed orientation tasks.

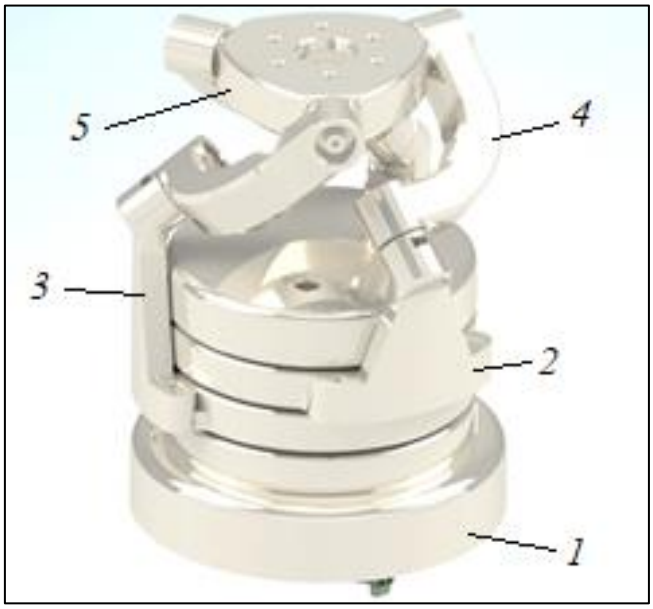

Fig 1: The structure of a 3-DOF spherical parallel manipulator with a 3-RRR and coaxial actuated input joint: 1-Base; 2-Rotary plate; 3-Proximal link; 4- Distal link; 5- Wrist.

The mechanical system under consideration is a robot leg belonging to a three-degree-of-freedom (3-DOF) spherical parallel manipulator (SPM) with a 3-RRR configuration and a coaxially actuated input joint (Figure 2).

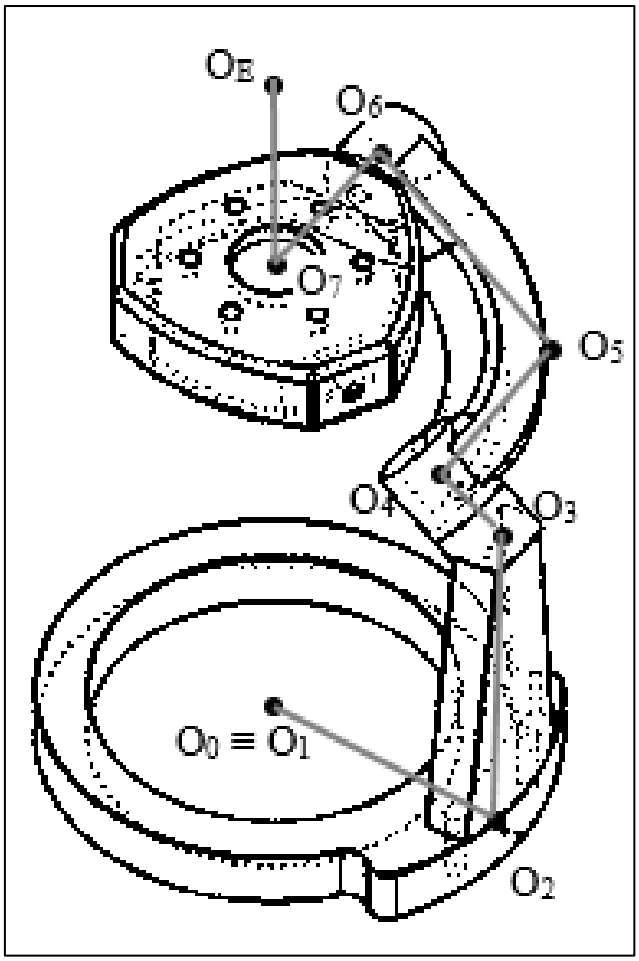

Fig 2: Preliminary description of the mechanical system of a robot leg in a 3-DOF spherical parallel manipulator with a 3-RRR structure and a coaxially actuated input join

A detailed kinematic model of the mechanical system is constructed as illustrated in Figure 3, which serves as the basis for subsequent derivations of the forward and inverse kinematic equations. This model is formulated by systematically assigning reference frames to each critical joint and link of the spherical parallel manipulator, and by establishing their relationships through homogeneous transformation matrices. Such a procedure ensures a consistent and rigorous mathematical description of the system's geometry and motion.

To begin with, a fixed coordinate system, denoted as $(OXYZ)_0$, is attached to the ground and defined as the global reference frame. This frame provides a stable origin for describing the spatial relationships of all subsequent moving parts of the mechanism. From this initial global frame, local coordinate systems are successively defined on each joint and link. These local frames are related to one another by a well-defined sequence of transformations that capture both translational and rotational displacements.

The first transformation, from $(OXYZ)_0$ to $(OXYZ)_1$, is described as a pure rotation about the OZ-axis through an angle of $(q_1+\pi/2)$. This operation represents the actuation of the first input joint, where q_1 is the corresponding generalized coordinate. The second transformation, from $(OXYZ)_1$ to $(OXYZ)_2$, consists of a translation along the OY -axis by a distance of $-a_1$. This translation effectively positions the subsequent frame relative to the offset introduced by the manipulator's base geometry.

Proceeding further, the transformation from $(OXYZ)_2$ to $(OXYZ)_3$ includes two operations: a translation along the OZ-axis by d_2, followed by a fixed rotation about the Ox-axis through an angle of $50°\sim(5\pi/18)$. This combined transformation accounts for the spatial displacement and inclination imposed by the manipulator's structural configuration.

Next, the transformation from $(OXYZ)_3$ to $(OXYZ)_4$ is described by a translation along the Oz-axis by d_3, combined with a rotation about the Oz-axis through an angle of $(q2-\pi/2)$. Here, q2 represents the second actuated joint variable, thus introducing an additional degree of freedom in the spherical motion of the system. The subsequent transformation, from $(OXYZ)_4$ to $(OXYZ)_5$, involves a translation along the Oy-axis by a distance a_4, which compensates for the geometrical offset of the corresponding link.

From $(OXYZ)_5$ to $(OXYZ)_6$, the transformation includes a translation along the OZ-axis by d_5, coupled with a rotation about the OX-axis through an angle of $\pi/2$. This operation reorients the frame to properly align with the next moving component of the manipulator. Subsequently, the transformation from $(OXYZ)_6$ to $(OXYZ)_7$ is performed through a translation along the OZ-axis by d_6, followed by a rotation about the OZ-axis through an angle of $(q_3+5\pi/18)$. At this stage, the third actuated joint variable q_3 is introduced, completing the three independent inputs of the spherical parallel mechanism.

Finally, the transformation from $(OXYZ)_7$ to the end-effector coordinate system $(OXYZ)_E$ is achieved by two sequential operations: a rotation about the OX-axis through $-\pi/2$, and a translation along the OZ-axis by d_7. The resulting homogeneous transformation matrix precisely describes the orientation and position of the end-effector relative to the global frame, and therefore constitutes the fundamental expression of the manipulator's forward kinematics.

By systematically applying these transformations, the complete kinematic chain of the spherical parallel mechanism with coaxial actuated input joints is fully characterized. This representation not only provides a rigorous foundation for further analysis of velocity and acceleration but also facilitates the derivation of the Jacobian matrix (in subsequent studies) and the subsequent investigation of workspace characteristics, singularity conditions, and dynamic behavior of the robot.

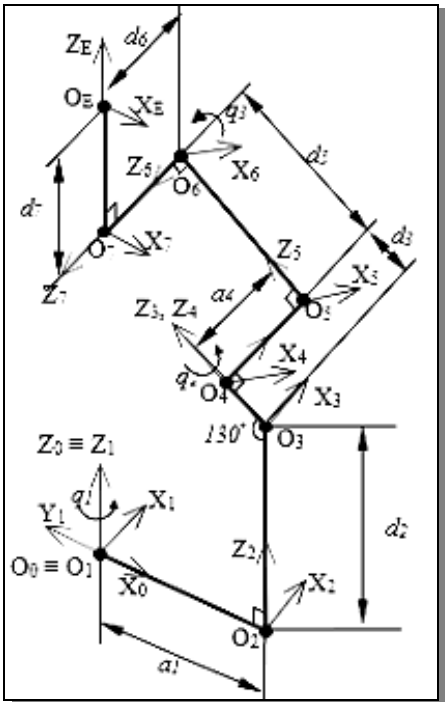

Fig 3: Kinematics diagram

To describe the kinematics of the robot through a combination of translations and rotations, homogeneous transformation matrices are employed, which are expressed in the general form given by Equation (1).

$$H_i = \begin{bmatrix} R_i & p_i \\ 0_{1\times 3} & 1 \end{bmatrix} \in SE(3), R \in SO(3), p \in \mathbb{R}^3. \quad (1)$$

Where SO(3) is Special orthogonal group in 3D$SO(3) = \{R \in \mathbb{R}^3 | R^T R = I, det(R) = +1\}$; SE(3) the set of 4×4 homogeneous matrices (rigid transformations in 3D space); d is translation vector$d \in \mathbb{R}^3$.
The matrix H_i represents the transformation of the $(OXYZ)_i$ coordinate frame with respect to the preceding frame $(OXYZ)_{i-1}$. Based on this, the local homogeneous transformation matrices are defined as follows.

$$H_1 = \begin{vmatrix} -sin(q_1) & -cos(q_1) & 0 & 0 \\ cos(q_1) & -sin(q_1) & 0 & 0 \\ 0 & 0 & 1 & 0 \\ 0 & 0 & 0 & 1 \end{vmatrix}; H_2 = \begin{vmatrix} 1 & 0 & 0 & 0 \\ 0 & 1 & 0 & -a_1 \\ 0 & 0 & 1 & 0 \\ 0 & 0 & 0 & 1 \end{vmatrix}$$

$$H_3 = \begin{vmatrix} 1 & 0 & 0 & 0 \\ 0 & cos\left(\frac{5\pi}{18}\right) & sin\left(\frac{5\pi}{18}\right) & 0 \\ 0 & -sin\left(\frac{5\pi}{18}\right) & cos\left(\frac{5\pi}{18}\right) & d_2 \\ 0 & 0 & 0 & 1 \end{vmatrix};$$

$$H_4 = \begin{vmatrix} sin(q_2) & cos(q_2) & 0 & 0 \\ -cos(q_2) & sin(q_2) & 0 & 0 \\ 0 & 0 & 1 & d_3 \\ 0 & 0 & 0 & 1 \end{vmatrix}$$

$$H_5 = \begin{vmatrix} 1 & 0 & 0 & 0 \\ 0 & 1 & 0 & a_4 \\ 0 & 0 & 1 & 0 \\ 0 & 0 & 0 & 1 \end{vmatrix}; H_6 = \begin{vmatrix} 1 & 0 & 0 & 0 \\ 0 & 0 & -1 & 0 \\ 0 & 1 & 0 & d_5 \\ 0 & 0 & 0 & 1 \end{vmatrix};$$

$$H_7 = \begin{vmatrix} sin\left(q_3 + \frac{2\pi}{9}\right) & cos\left(q_3 + \frac{2\pi}{9}\right) & 0 & 0 \\ -cos\left(q_3 + \frac{2\pi}{9}\right) & sin\left(q_3 + \frac{2\pi}{9}\right) & 0 & 0 \\ 0 & 0 & 1 & d_6 \\ 0 & 0 & 0 & 1 \end{vmatrix}; H_8 = \begin{vmatrix} 1 & 0 & 0 & 0 \\ 0 & 0 & 1 & l_7 \\ 0 & -1 & 0 & 0 \\ 0 & 0 & 0 & 1 \end{vmatrix}$$

By employing homogeneous transformation matrices, the pose of the $(OXYZ)_i$ frame relative to the fixed coordinate system $(OXYZ)_0$ can be determined as follows:

$$D_{0n} = \prod_{i=1}^{n} H_i, n = 8. \quad (2)$$

From this, the position of the end-effector coordinate frame E with respect to the fixed base frame can be expressed as follows, in which the coordinates of the end-effector x_E, y_E, z_E also represent the forward kinematic equations of the mechanism.

$$D_{0E} = \begin{vmatrix} r_{11} & r_{12} & r_{13} & x_E \\ r_{21} & r_{22} & r_{23} & y_E \\ r_{31} & r_{32} & r_{33} & z_E \\ 0 & 0 & 0 & 1 \end{vmatrix} \quad (3)$$

By using specialized computational software, we obtain the following results:

$$\begin{aligned} x_E &= l_7.\left(-Sq_1.Sq_2 + Cq_1.C\left(\frac{5\pi}{18}\right).Cq_2\right).C\left(q_3 + \frac{2\pi}{9}\right) - \\ &C(q_1).S\left(q_3 + \frac{2\pi}{9}\right).S\left(\frac{5\pi}{18}\right).l_7 - Cq_1.Sq_2.(a_4 - d_6).C\left(\frac{5\pi}{18}\right) \\ &- Cq_1.(d_3 + d_5).S\left(\frac{5\pi}{18}\right) + Cq_1.a_1 - Cq_2.Sq_1.(a_4 - d_6) \end{aligned} \quad (4)$$

$$y_E = l_7.\left(Cq_1.Sq_2 + Sq_1.C\left(\frac{5\pi}{18}\right).Cq_2\right).C\left(q_3 + \frac{2\pi}{9}\right) - Sq_1.S\left(q_3 + \frac{2\pi}{9}\right).S\left(\frac{5\pi}{18}\right).l_7 - Sq_1.Sq_2.(a_4 - d_6).C\left(\frac{5\pi}{18}\right) - Sq_1.(d_3 + d_5).S\left(\frac{5\pi}{18}\right) + Sq_1.a_1 + Cq_1.Cq_2.(a_4 - d_6) \quad (5)$$

$$z_E = Cq_2.C\left(q_3 + \frac{2\pi}{9}\right).S\left(\frac{5\pi}{18}\right).l_7 + C\left(\frac{5\pi}{18}\right).S\left(q_3 + \frac{2\pi}{9}\right).l_7 + (d_3 + d_5).C\left(\frac{5\pi}{18}\right) - Sq_2.(a_4 - d_6).S\left(\frac{5\pi}{18}\right) + d_2 \quad (6)$$

2.2. Workspace description

The workspace of a serial robot is the set of all positions and that the end-effector (EE) can reach, given the joint constraints. In this study, we only need to consider the positional workspace, where the orientation of the end-effector is defined as the direction from the center of rotation to the positions obtained within the workspace. The reachable workspace of the end-effector is represented as follows:

$$W_P = \{X(q) \in \square^3 \mid q \in Q\}$$

with:

- $Q = \{q \in \mathbb{R}^n | {q_i}^{min_{ii}}{}^{max}\}$ is joint space domain.
- $X(q) = [x(q), y(q), z(q)]^T$ is end-effector position.

3. Results and Debates

3.1. The Forward Kinematics Problem

Based on the predetermined geometric parameters of the robot leg that is intended to be designed and manufactured, the fundamental dimensions of the mechanism can be specified as follows: $d_1 = 0.1215$, $d_2 = 0.1858$, $d_3 = 0.035$, $a_4 = 0.1008$, $d_5 = 0.1236$, $d_6 = 0.1008$, $l_7 = 0.120$. These parameters represent the essential link lengths and offsets that characterize the geometry of the spherical parallel robot leg under investigation. In particular, the values of d_1, d_2 and d_3 correspond to the distances defining the relative positions of the joints along the input axis, while a_4 specifies a crucial lateral displacement that determines the spatial configuration of the intermediate link. Similarly, d_5 and d_6 describe the subsequent offsets that directly influence the overall shape of the mechanism, and l_7 represents the effective length of the terminal link connecting to the moving platform.

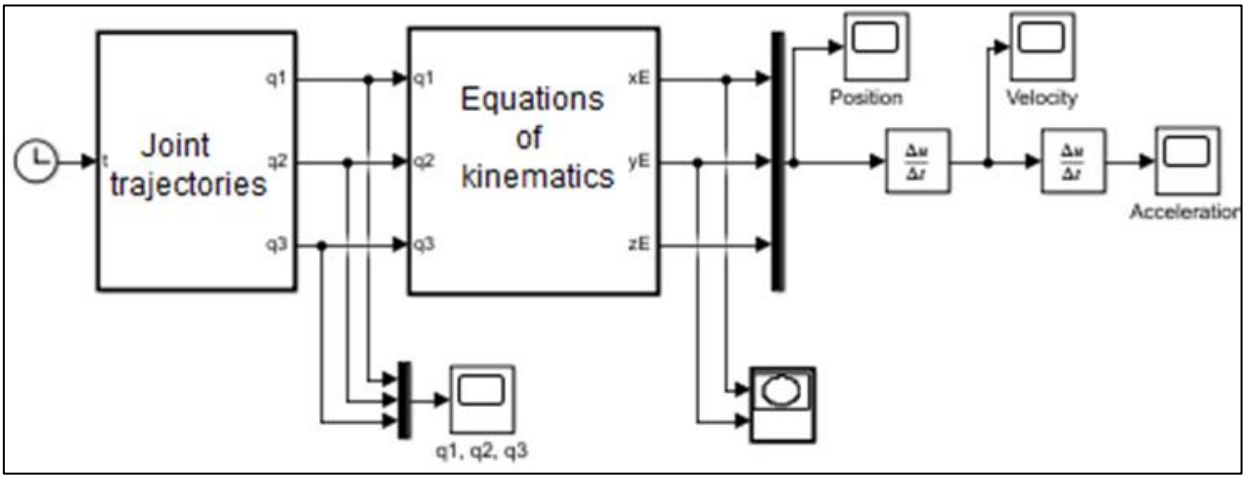

Fig 4. Forward kinematics calculation diagram

The forward kinematics problem is formulated with the input being the motion law of the joint variables and the output being the motion law of point E (or any point on the mechanism) within the workspace, including its position, velocity, and acceleration. This problem can be solved using MATLAB computational software, following the schematic representation in Figure 4.

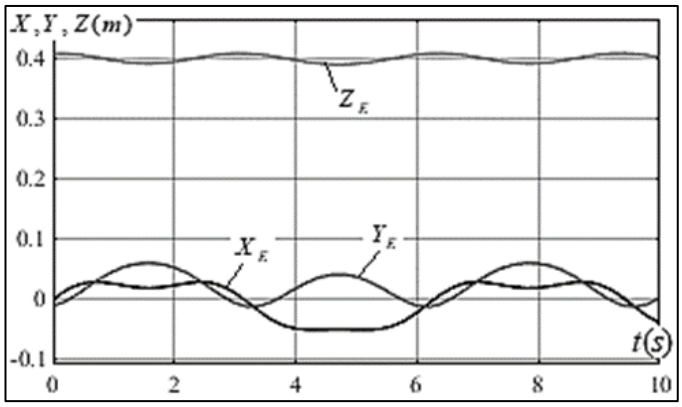

Fig 5: The law of variable joints

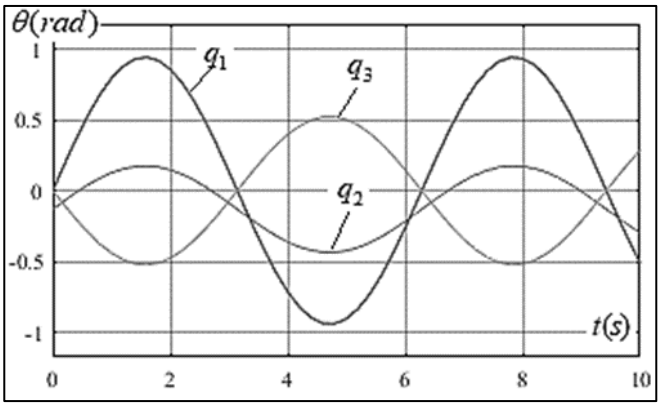

Fig 6: Position of E point

The forward kinematics problem is formulated with the input being the motion law of the joint variables $q_1(t) = (3\pi/10)\,sin(t)$, $q_2(t) = \pi/12 + (\pi/36).sin(t)$, $q_2(t) = (-\pi/6).sin(t)$ and the output being the motion law of point E (or any point on the mechanism) within the workspace, including its position, velocity, and acceleration. This problem can be solved using MATLAB computational software, following the schematic representation in Figure 5.

The outcomes of the analysis are illustrated in Figures 6 through 9. Figure 6 depicts the position of point E, where the maximum displacement along the $(OZ)_E$ axis reaches 0.42 m, while along the $(OX)_E$ and $(OY)_E$ axes it attains 0.028 m and 0.06 m, respectively. Figures 7 and 8 present the velocity and acceleration profiles of point E, respectively.

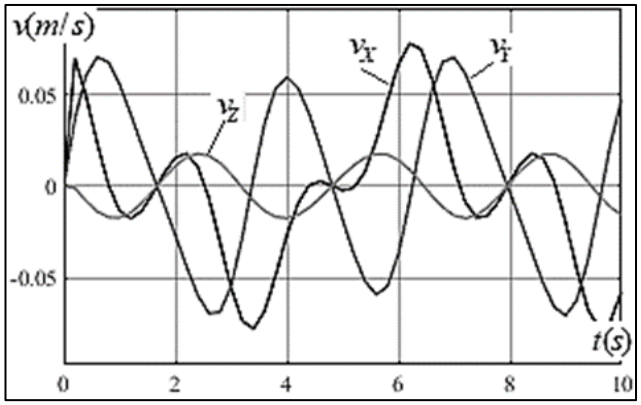

Fig 7: Velocity of E point

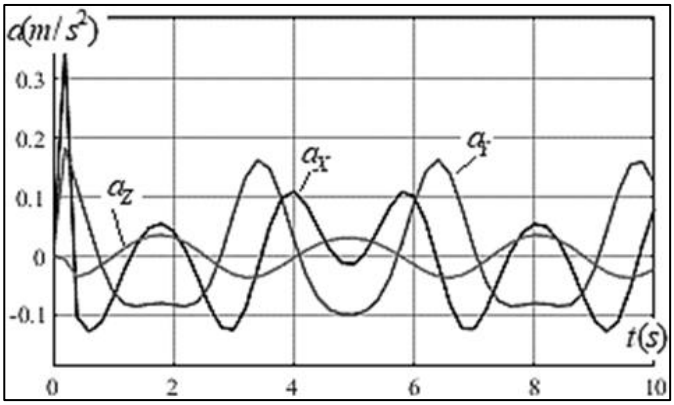

Fig 8: Acceleration of E point

3.2. Workspace of the end-effector

From the geometric structure of the mechanism, it can be inferred that the admissible range of motion for each actuated joint is restricted by specific joint limits, which are expressed as follows: $-3\,\pi/10 \le q_1 \le 3\pi/10$, $\pi/9 \le q_2 \le \pi/18$, $-\pi/6 \le q_3 \le \pi/6$.. These inequalities define the feasible angular displacements of the joints, ensuring that the mechanism operates within its physical and mechanical constraints. In practical terms, the limits of q_1, q_2, and q_3 reflect the maximum permissible rotations that can be achieved without causing structural interference, overstressing the links, or exceeding the allowable range of the actuators.

Based on these constraints, the attainable region of the moving platform, i.e., the workspace of the end-effector, can be systematically derived. This workspace represents the set of all possible positions and orientations that the end-effector can achieve when the joint variables vary within the aforementioned ranges. It provides a comprehensive geometric description of the robot's operational capabilities and serves as a crucial basis for evaluating the performance of the mechanism in practical applications. The calculated workspace is illustrated in Figure 9, where the boundaries correspond to the extreme values of the joint limits. Such representation not only highlights the feasible operating domain but also enables comparison with desired task requirements, thereby confirming the suitability of the proposed design for its intended function.

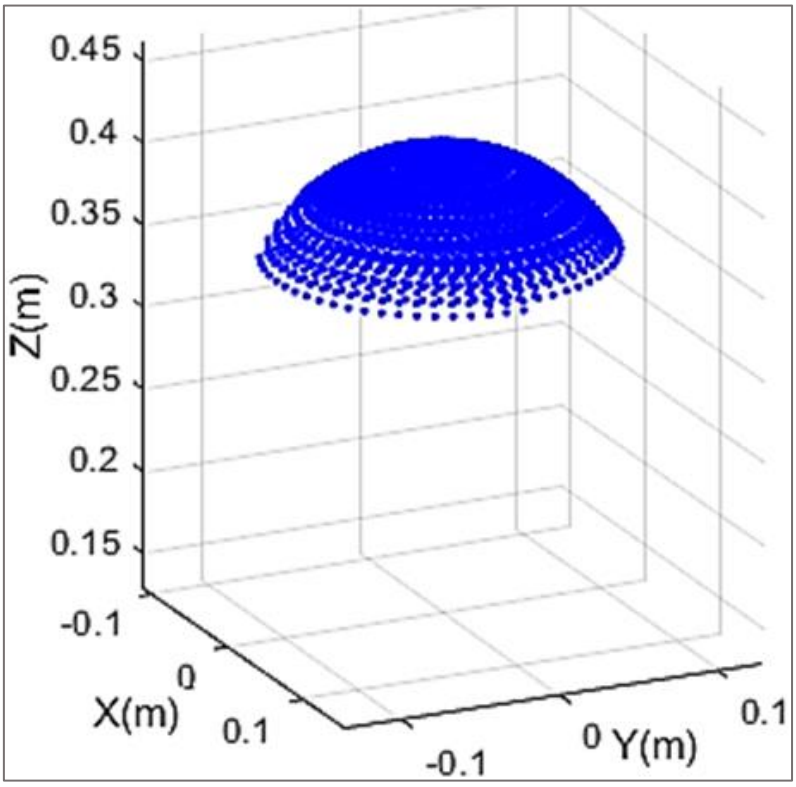

Fig 9: Workspace of the end-effector (E)

4. Conclusions

This paper has systematically developed the forward kinematic and inverse dynamic models for a single leg of a 3-DOF spherical parallel robot with coaxial input links—a configuration that is both practically relevant and rarely detailed in the literature. The homogeneous transformation matrix approach enables precise description of the mechanism's motion, while the inverse dynamic formulation allows the determination of torques at both actuated and passive joints. This reveals the transmission of forces through the links and clarifies the effects of inertia, Coriolis/centrifugal forces, and gravity on the overall dynamics. Characterizing joint torques not only supports the analysis and validation of the equations of motion but also establishes a solid foundation for design optimization, improved transmission efficiency, and the development of advanced control strategies. The outcomes presented herein provide a significant scientific basis for extending toward full-system modeling and practical deployment of spherical parallel robots in applications demanding high precision and reliability.

5. References

1. Bai S, Hansen MR, Angeles J. A robust forward-displacement analysis of spherical parallel robots. Mech Mach Theory. 2009;44(12):2204-16. doi:10.1016/j.mechmachtheory.2009.07.005
2. Nigatu H, Lihao J, Shi G, Lu G, Dong H. Unveiling the complete variant of spherical robots. arXiv preprint arXiv:2403.03505. 2024.
3. Cruz-Reyes AT, Arias-Montiel M, Tapia-Herrera R. Kinematic analysis of a coaxial 3-RRR spherical parallel manipulator based on screw theory. In: Zeghloul M, Laribi M, Arsicault M, editors. Mechanism design for robotics. Cham, Switzerland: Springer; 2021. p. 28-37. doi:10.1007/978-3-030-75271-2_4
4. Bai S, Hansen MR, Andersen TO. Modelling of a special class of spherical parallel manipulators with Euler parameters. Robotica. 2009;27(2):161-70. doi:10.1017/S0263574708004402
5. Khang NV, My CA. Industrial robotics fundamentals. Hanoi, Vietnam: Science and Technology Publishing House; 2023.
6. Dinc HT, Hulin T, Rothammer M, Seong HS, Willberg B, Pleintinger B, Ryu JH, Ott C. CoaxHaptics-3RRR: a novel mechanically overdetermined haptic interaction device based on a spherical parallel mechanism. In: Proc. 2024 IEEE Conf. Telepresence (Telepresence 2024); 2024 Nov; Pasadena, CA, USA. IEEE; 2024. p. 87-94. doi:10.1109/Telepresence63209.2024.10841776
7. Gosselin CM, Pierre ES, Gagne M. On the development of the Agile Eye. IEEE Robot Autom Mag. 1996;3(4):29-37.
8. Wu G, Bai S. Design and kinematic analysis of a 3-RRR spherical parallel manipulator reconfigured with four-bar linkages. Robot Comput Integr Manuf. 2019;56:55-65.
9. Gosselin C, Angeles J. The optimum kinematic design of a spherical three-degree-of-freedom parallel manipulator. J Mech Transm Autom Des. 1989;111(2):202-7.
10. Wu G. Multiobjective optimum design of a 3-RRR spherical parallel manipulator with kinematic and dynamic dexterities. Model Identif Control. 2012;33:111-22.
11. Steiner W. Modélisation cinématique et simulation d'un robot rotule à 3 degrés liberté à très haute dynamique. Lausanne: HES-SO; 2015.
12. Rodriguez J, Ruggiu M. Analytical solution of the forward displacement problem for spherical parallel manipulators.

Berkeley, CA and Cagliari, Italy: University of California at Berkeley and University of Cagliari; 2012.
13. Mulan W, Xiaoxia L, Kaiyun X, Rong J. Smooth trajectory planning for manipulator of cotton harvesting machinery based on quaternion and B-spline. In: International Symposium on Instrumentation & Measurement, Sensor Network and Automation (IMSNA); 2012. p. 134-7.
14. Bu S, Yan L, Gao X, Wang G, Zhao P, Chen IM. Design and motion control of spherical robot with built-in four-wheel omnidirectional mobile platform. IEEE Trans Instrum Meas. 2023;72:1-10.
15. Zhang Y, Zhang L, Wang W, Li Y, Zhang Q. Design and implementation of a two-wheel and hopping robot with a linkage mechanism. IEEE Access. 2018;6:42422-30.
16. Tursynbek I, Niyetkaliye A, Shintemirov A. Computation of unique kinematic solutions of a spherical parallel manipulator with coaxial input shafts. In: Proc. IEEE 15th Int. Conf. Autom. Sci. Eng. (CASE); 2019 Aug. IEEE; 2019. p. 1524-31.
17. Howard IS. Design and kinematic analysis of a 3D-printed 3DOF robotic manipulandum. In: Proc. Annu. Conf. Towards Auto. Robotic Syst.; 2023. p. 227-39.